Quantum Electronics 47 (6) 503 – 508 (2017) ©2017 Kvantovaya Elektronika and Turpion Ltd

https://doi.org/10.1070/QEL16382

Modification of the SiO_2/Si interface by pulsed fibre laser radiation*

A.M. Skvortsov, V.P. Veiko, C.T. Huynh, D.S. Polyakov, A.M. Tamper

Abstract. **We report a detailed study of structural modification of the silicon – silica interface under the effect of laser pulses at a wavelength of 1.07 μm. A thermal oxide layer on the silicon surface has been shown to have a significant effect on the defect formation process and surface microstructuring because of the complex stress state of such a structure.**

Keywords: *silicon – silica interface, microstructuring, dislocations, micromelting, fibre laser.*

1. Introduction

The influence of laser irradiation on silicon has been the subject of extensive studies. Research interest in this issue is due in many respects to the possibility of producing various surface microtopographies on silicon, capable of drastically changing its surface properties. For example, previous results [1 – 3] demonstrate the possibility of laser-induced surface texturing, with a considerable reduction in the optical reflectivity of the material (so-called black silicon), which can be used to raise the efficiency of solar cells. In addition, laser microstructuring of silicon makes it possible to produce superhydrophobic [4] or superhydrophilic [5] surfaces. Considerable attention is paid to the study of laser-induced periodic surface structures originating from the interaction of incident light with surface plasmon polaritons [6, 7].

Another research direction is concerned with the influence of laser irradiation on the defect density in semiconductors. One well known technology is pulsed laser annealing, which is used e.g. to remove structural defects and imperfections produced by ion implantation into the surface layer of silicon [8]. On the other hand, laser irradiation may produce structural defects in silicon [9]. It is important to note that the generation and growth rates of such defects are influenced not only by the incident light intensity but also by the way it is distributed over the exposed area and the pulse repetition rate [10]. At the same time, the presence of certain defect species in silicon can be used for obtaining new effects and making new classes of devices. For example, it is well known that, being an indirect gap semiconductor, pure single-crystal silicon is poorly suited for the fabrication of light-emitting devices because of the low probability of radiative transitions in it. However, the presence of structural defects can be favourable for efficient luminescence in silicon [11, 12]. Thus, the ability to control defect density in silicon exposed to laser radiation is a topical issue in microelectronics and optoelectronics.

In this connection, we think that there is particular interest in the study of the influence of laser irradiation on the silicon – silica system. Note, first of all, that it is the SiO_2/Si structure which lies at the core of modern microelectronic devices. Moreover, the silicon – silica interface possesses a variety of physical features that have a significant effect on defect formation and structuring processes. These features include the high transmission of silica at optical wavelengths and the lattice, thermal expansion and elastic mismatch. They may lead to the generation of considerable additional mechanical stress under laser irradiation and require detailed investigation.

The specifics of the issue in question shows up most clearly in the visible and near-infrared spectral regions at a sufficiently short pulse duration and high pulse repetition rate. From this point of view, the light source best suited for such studies is a pulsed ytterbium fibre laser. Additional interest in this issue is aroused by the considerable potential of fibre lasers for industrial applications and the fact that their effect on the structure under consideration has been poorly studied. Some results in this area of research were reported previously [10, 13 – 15]. In particular, attention was paid to active dislocation generation under the effect of a laser pulse train, and taking into account thermal stress was shown to be of general importance in this case.

In the context of the above, the objectives of this report are to present new results of our research into the structural modification of the silicon – silica interface under the effect of pulsed ytterbium fibre laser radiation at a wavelength of 1.07 μm and to systematise the key features of the modification related to the presence of a thermal oxide layer, different distributions of irradiation spots over the substrate surface and the high pulse repetition rate.

2. Experimental

The samples used in our experiments were (100)-oriented KEF-4.5 (phosphorus-doped) and (111)-oriented KDB-10

*Presented at the Fundamentals of Laser-Assisted Micro- and Nanotechnologies (FLAMN-2016) International Symposium (Pushkin, Leningrad oblast, 27 June to 1 July 2016).

A.M. Skvortsov, V.P. Veiko, D.S. Polyakov, A.M. Tamper St. Petersburg National Research University of Information Technologies, Mechanics and Optics, Kronverkskii prosp. 49, 197101 St. Petersburg, Russia; e-mail: a-skvortsov@yandex.ru, veiko@lastech.ifmo.ru, polyakovdmitry1988@gmail.com, anton-t-@mail.ru;
C.T. Huynh Quy Nhon University, Quy Nhon, Viet Nam

Received 24 March 2017
Kvantovaya Elektronika **47** (6) 503 – 508 (2017)
Translated by O.M. Tsarev

(boron-doped) single-crystal silicon wafers. A silica layer was grown in humid oxygen at a temperature of 1000 °C. Its thickness was 40, 150 and 500 nm in different samples. In addition, we used single-crystal silicon wafers that were not thermally oxidised and had a native silica layer of the order of 4 nm in thickness.

As a laser source, we used a repetitively pulsed ytterbium fibre laser with the following characteristics: average output power, up to 50 W; pulse repetition rate, 20–100 kHz; pulse duration, 100 ns. The laser beam was scanned over the wafer surface by a 2D laser beam scanner at a speed of up to 8000 mm s^{-1}. Irradiation conditions were adjusted so as to avoid ablation and maintain the oxide layer intact. We used different spot distributions over the exposed surface: without beam scanning (single-shot regime and multiple-shot exposure at a high pulse repetition rate) and with scanning. In the case of single-spot, multiple-shot laser exposure of the SiO_2/Si structure, we used a defocused laser beam. If the irradiation zone was produced by scanning the laser beam, the scan conditions were adjusted so that the spots severely overlapped.

After irradiation, the samples were characterised by optical and probe microscopies. Their electrical characteristics were determined by high-frequency (ω = 1 MHz) capacitance–voltage ($C-V$) measurements using the following contact configuration: a four-probe contact to the (unoxidised) backside of the wafer and an InGa-coated tungsten probe on the oxidised side.

3. Silicon–silica interface reconstruction during laser exposure

Surface reconstruction is a process in which surface atoms of a crystal change their positions compared to the bulk of the material so that the resulting surface structure differs in periodicity and/or symmetry from the bulk. In theory, there are a variety of reconstructed silicon surface geometries. The Si(111) surface typically has (2×1) and (7×7) structures [16]. This surface can also have (5×5), (3×3) and (9×9) structures, depending on heat treatment temperature. The Si(100) surface typically has (2×1) and (4×2) reconstructions [17].

Given that structural defects play a special role in the laser microstructuring of silicon and the silicon–silica system, the purpose of our experiments was to find out how the initial surface reconstruction of a silicon wafer influences its microstructuring behaviour under laser irradiation.

In our SiO_2/Si microstructuring experiments, we used a laser system based on the pulsed ytterbium fibre laser described above. The incident power density was 1.2×10^7 W cm^{-2} at an oxide thickness of 150 or 40 nm and 2.0×10^7 W cm^{-2} at an oxide thickness of 500 nm. The beam diameter in the plane of irradiation was 50 μm, and the samples were exposed to single pulses. An essential point is that the irradiation conditions chosen allowed the SiO_2 film to remain intact. Typical SiO_2/Si interface microstructuring results are presented in Fig. 1.

In all the wafers, the SiO_2/Si interface had characteristic microstructures in the laser irradiation zone. The irradiated regions resembled a 'flower', with a circular zone in its centre and 'petals' around it. The number of petals varied from region to region. After irradiation of the (111)-oriented wafer (Fig. 1a), the average number of petals was seven. On the (100)-oriented wafers, the number of petals reached ten. After irradiation of the (111)-oriented wafer with an oxide thickness d_o = 40 nm, the irradiated regions had no well-defined topological forms, and structures similar to those in Fig. 1a were only slightly discernible on the wafer surface. However, irradiation of these structures at higher power densities did not improve the contrast and lead to disintegration of the SiO_2 films, followed by silicon ablation. On the samples having a native silica layer, no petal structures were detected. Analysis of the morphology of the observed structures indicated that the modified regions consisted of single-crystal silicon crystallized after micromelting in separate portions of the irradiated regions. After the SiO_2 film was removed by etching in hydrofluoric acid and the wafers were rinsed, the silicon surface in the irradiated regions perfectly reproduced the microtopography of the SiO_2/Si system.

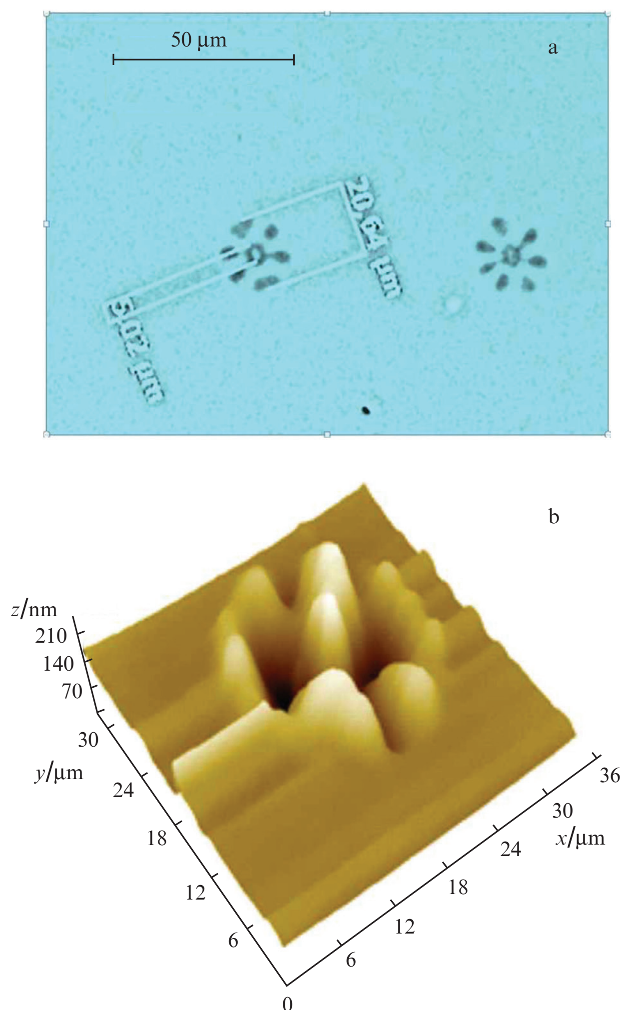

Figure 1. (a) Micrograph and (b) AFM image of an irradiated region on the SiO_2/Si interface of a (111)-oriented silicon wafer; oxide thickness d_o = 150 nm; incident power density, 1.2×10^7 W cm^{-2}.

The (7×7) reconstruction geometry can be described by a dimer–adatom–stacking fault (DAS) model [18]. Without going into the details of the DAS model from the crystallographic point of view, it should be noted that it is surface reconstruction that leads to a symmetric arrangement of structural defects in the top surface layer of silicon. It is also responsible for symmetric micromelting patterns in the irradiated regions. It seems likely that it is the rhomboid structure of the DAS model, which forms a 'sublattice' of the surface silicon layer, that determines the stably symmetric topology of the irradiated regions, which is independent of the surface

orientation of the silicon wafers and their conductivity type. The only distinction is that the number of petals in the irradiated region depends significantly on the crystallographic orientation of the silicon substrate surface.

Figure 1b shows a 3D AFM image illustrating the surface topography of an irradiated region in the SiO_2/Si system after irradiation of a (111)-oriented wafer with a SiO_2 thickness d_o = 150 nm. It is seen that the nanotopography is formed by 130-nm-high tapered columns surrounding a 260-nm-high central column. They consist of a solidified silicon melt covered with thin ('stretched') SiO_2 film, whose thickness decreases towards the top of the columns.

4. Formation of a slip line network on the silicon–silica interface

This series of experiments was aimed at gaining insight into the mechanisms responsible for the laser microstructuring of the SiO_2/Si system and related to active defect generation and plastic deformation of near-surface atomic silicon layers adjacent to the SiO_2 layer.

In our experiments, we used single-spot irradiation of the SiO_2/Si structure with a series of pulses at a repetition rate of 50 kHz, beam diameter in the plane of irradiation near 1 mm, irradiation time of 15 s and average output power of 45 W. The sample was placed on a massive copper substrate. As in the preceding experiments, the wafers were irradiated from the oxidized side and the light was absorbed on the silicon surface.

Figure 2a shows a dark-field micrograph of irradiated samples. It is seen that, within the irradiated surface region, there is an ordered network of slip lines, which are outcrops of line dislocations moving on crystallographic slip planes towards the SiO_2 film. This leads to the formation of surface steps whose height is determined by the number of dislocations that have outcropped on a given slip plane.

On the (100)-oriented samples, the lines intersect at 90°; on the (111)-oriented samples, at 60°. We failed to obtain such structures on pure (unoxidized) silicon samples.

Figure 3 shows AFM images of a slip band in the central part of the micrograph presented in Fig. 2a. It is seen that the height of the steps formed by slip lines can reach several tens of nanometres.

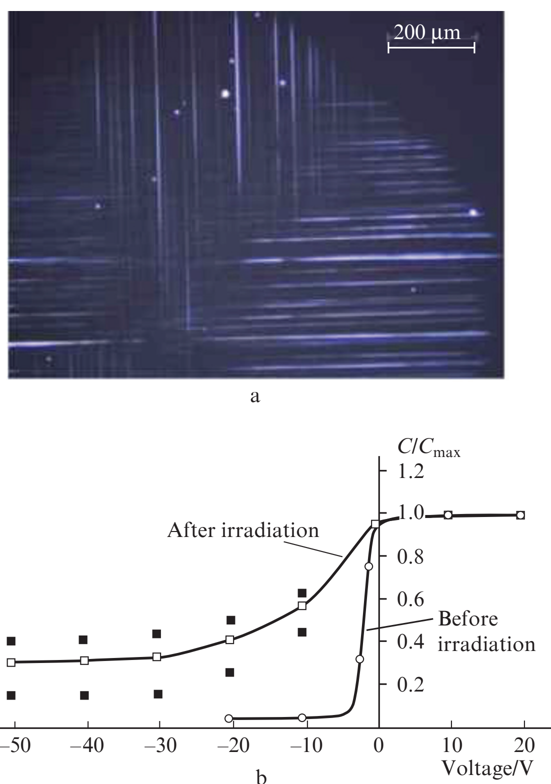

Figure 2. (a) Micrograph of an irradiated region on the SiO_2/Si interface of a (100)-oriented silicon wafer (with slip lines) and (b) the corresponding capacitance–voltage curves; d_o = 150 nm.

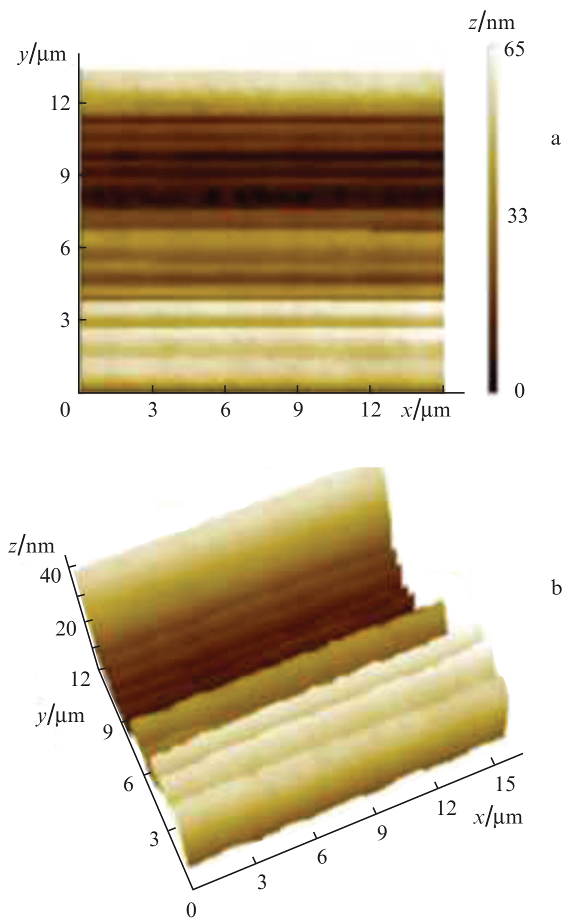

Figure 3. (a) 2D and (b) 3D AFM images of a slip band.

The conditions under which the structures shown in Fig. 2a were produced were chosen for the following reasons: First, the incident power density should not exceed the melting threshold of silicon, which is ensured by the sufficiently large beam diameter (~1 mm) in the irradiation zone due to beam defocusing. Second, the defect generation process has an accumulative character, so we used a rather long irradiation time (~10 s) at high pulse repetition rates (~100 kHz). In our opinion, these conditions are optimal for rapid generation of defects (including dislocations) and effective manifestation of a slip line network on the sample surface during plastic deformation.

The above results indicate that laser irradiation of the SiO_2/Si system considerably increases the dislocation density

in it. The laser heating-induced stress leads to plastic deformation, accompanied by dislocation motion. Outcropping dislocations produce a slip line network similar to that in Fig. 2a (its appearance is determined by the crystallographic orientation of the sample). It is important to note that it is the SiO_2/Si interface which is responsible for the formation of numerous low-energy dislocation nucleation centres.

The accumulation of structural defects (native point defects and dislocations) is a gradual process, whereas the formation of a slip line network is a very fast process that occurs when a certain critical laser fluence is reached. At the initial instant, the slip line network has a very high density of ultrafine lines. Increasing the laser fluence (the number of pulses) increases the thickness of the slip lines and the spacing between them. A further increase in the number of pulses leads to the nucleation of microcracks, which then grow into the bulk of the crystal. The microcracking process ends with the formation of a small microcrack 'star' on the backside of the silicon wafer, which corresponds to the surface orientation and is centred in the middle of the irradiated region. Finally, a still further increase in the number of pulses leads to cracking of the silicon wafer.

Special mention should be given to the role of the silica layer in the SiO_2/Si system in these experiments: it produces considerable tensile shear stress and acts as a source of nucleation centres for structural defects in the surface layer of the silicon.

Figure 2b shows $C-V$ curves (normalised to the maximum capacitance) for the irradiated regions whose micrographs are presented in Fig. 2a. In all cases, we observe significant changes in capacitance–voltage behaviour. In the voltage range corresponding to the transition from accumulation to inversion, the slope of the $C-V$ curve changes for the samples of both conductivity types, attesting to a change in the density of surface states across the silicon–silica interface. A shift of the $C-V$ curve along the voltage axis, indicating a change in the oxide charge, is only observed for the p-type sample. Breakdown voltage measurements for our samples detected no significant variation from the initial level.

Thus, the present experimental data on the microstructuring of the SiO_2/Si system demonstrate that the formation of various structural defects, including dislocations, in the surface layer of silicon may cause slip lines to emerge. Owing to specific features of the crystal structure of silicon single crystals, the resultant slip line network allows one to determine the crystallographic orientation of the silicon wafer. Moreover, the proposed method of microstructuring the silicon surface in the SiO_2/Si system can be used for the fabrication of high-resolution atomic gratings.

5. Kinetics of silicon micromelting on the SiO_2/Si interface

Special attention should be paid to silicon melting processes on the surface adjoining the thermal silica layer. Even in the initial state, the surface silicon layer in the SiO_2/Si system suffers high mechanical stress, which stretches the crystal lattice. Under the effect of laser irradiation, silicon micromelting localises around outcrops of structural defects, including dislocations. It is reasonable to assume that micromelting localisation centres in this experiment are the surface regions where silicon substrate reconstruction processes took place before and during thermal oxidation. In these surface areas of the crystal lattice, the covalent bonds between atoms are weaker because of the displacement of the atoms from their lattice sites.

Micromelting on the silicon surface in the centre of the laser spot can be accounted for by the higher laser fluence in this part of the spot. This leads to a greater melting depth and greater height of the crystallised silicon region in the centre of the irradiated region. In the regions that are here referred to as petals (Fig. 1), micromelting occurs where reconstruction takes place not only in the surface layer (the presence of 'subplanes') but also deeper in the silicon crystal, extending to a number of atomic planes where the covalent bonds between atoms are also weaker because of the presence of stacking faults. The melting depth is here smaller than in the centre of the irradiated region and the crystallised silicon columns are lower. Note that we should also take into account specific features of interaction between softened SiO_2 film and molten silicon.

In our experiments, we detected local (point) micromelting within the irradiation zone at temperatures below the melting point of silicon In at point-defect accumulations. It is important to note that such an effect was also observed when the oxide film was intact.

In those experiments, the samples were irradiated at various beam scanning speeds, with overlapping irradiation spots, which allowed us to smoothly control the temperature in the irradiation zone and examine structure modification under irradiation conditions near the melting threshold. We used a convergent beam with an average power of 50 W. The pulse repetition rate was 50 kHz and the beam diameter in the plane of irradiation was 300 μm.

Figure 4 shows surface micrographs of thermally oxidized (111)-oriented silicon after laser irradiation at different beam scanning speeds. It is seen that high beam scanning speeds lead to the formation of submicron-sized melting zones on the silicon surface. Reducing the scanning speed increases the density of dislocations and new melting centres and the surface area of the already existing melting centres. At a scanning speed of 60 mm s^{-1}, the linear dimensions of the local melting zones reach 4–5 μm and the corresponding recrystallization regions become triangular in shape (Fig. 4d).

The shape of equilateral triangles on the surface of silicon is known to be typical of anisotropic chemical etch pits at the points of outcrop of dislocations on the (111) surface. In our case, like chemical etching, silicon melting occurred at points of outcrop of laser irradiation-induced dislocations on the surface of the silicon substrate. As mentioned above, an important role in the generation of structural defects, including dislocations on the silicon surface, is played by the silica layer. Local micromelting in dislocation outcrop regions is possible as well on substrates having a native oxide layer, but this requires multiple scanning of a given region. After the surface SiO_2 layer is removed by etching, the surface of the recrystallized layer perfectly reproduces the morphology of the SiO_2/Si system.

Thus, the present experimental data lead us to conclude that basic to the mechanism behind the formation of local microregions of molten silicon (anisotropic silicon micromelting) under pulsed laser irradiation are dislocation phenomena. A sequence of nanosecond laser pulses leads to the generation and accumulation of dislocations near the SiO_2/Si interface. The resulting stress causes plastic deformation, and dislocations outcrop in the deformed regions. It is around the dislocation outcrops that micromelting occurs.

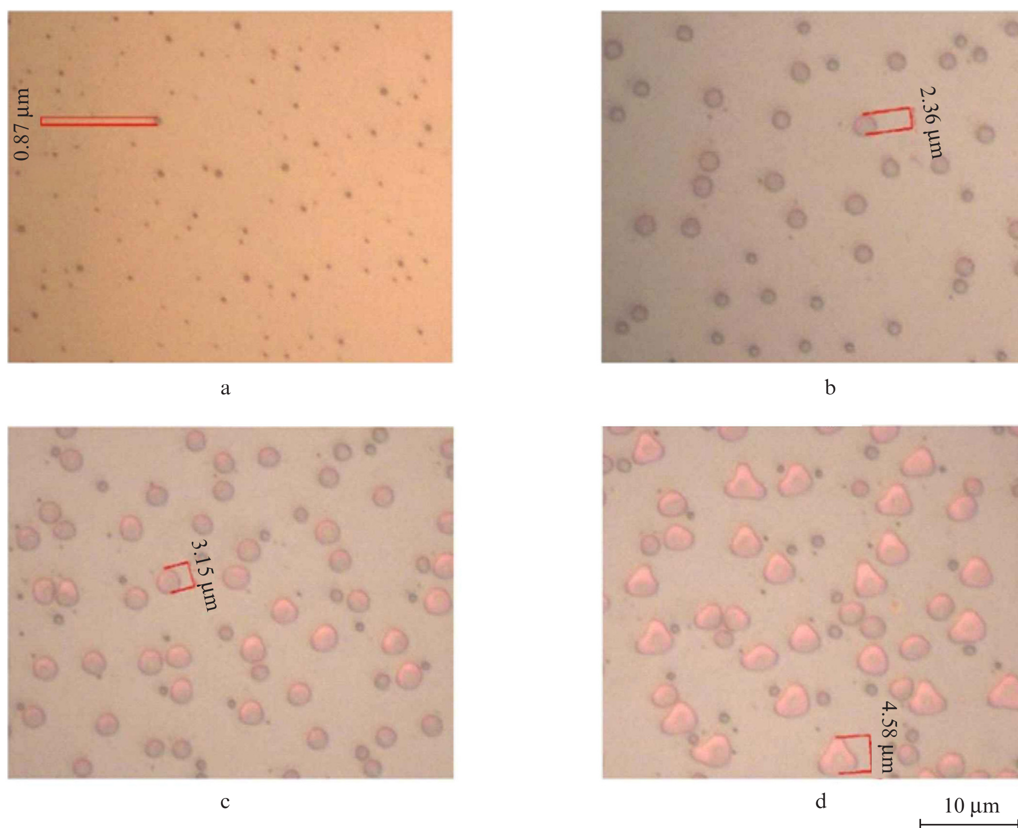

Figure 4. Micrographs of regions irradiated at beam scanning speeds of (a) 100, (b) 80, (c) 70 and (d) 60 mm s^{-1}.

6. Conclusions

In this paper, we have presented main results of our research into the laser microstructuring of single-crystal silicon wafers having silica films (SiO_2/Si structures) produced by high-temperature thermal oxidation. An important role in silicon surface modification experiments is played by the presence of a SiO_2 film on the silicon surface. Because of this, all our experiments were carried out under conditions that allowed the SiO_2 film to remain structurally intact and the silicon wafer to remain single-crystalline. Under such conditions, we obtained a number of interesting results.

Using single-shot microstructuring of the SiO_2/Si system with a fibre laser, we have obtained for the first time patterns that provide indirect insight into the surface reconstruction of the silicon substrate before thermal oxidation. The morphology of the resultant microstructures is determined by the combined effect of a number of factors: crystallographic orientation of the wafer, initial surface reconstruction of the wafer, elastic mechanical stress in the SiO_2/Si system and laser radiation.

We have detected local plastic deformation of the silicon surface in the form of a slip line network as a result of the exposure of the SiO_2/Si system to fibre laser pulses. The shape of the slip line network depends on the principal crystallographic orientation of the silicon substrate. Such surface modification is accompanied by changes in the electrical properties of the system.

We have experimentally demonstrated that laser beam scanning can cause local anisotropic micromelting of single-crystal silicon at a temperature below its melting point. The formation of local microregions of molten silicon under the oxide layer during laser irradiation at a high pulse repetition rate has been shown to be mainly due to a dislocation mechanism: rapid generation and accumulation of defects.

Acknowledgements. This work was financially supported by the RF Ministry of Education and Science [Agreement No. 14.578.21.0197 (RFMEFI57816X01970)].

References

1. Vorobyev A.Y., Guo C. *Appl. Surf. Sci.*, **257**, 7291 (2011).
2. Sarnet T., Halbwax M., Torres R., Delaporte P., Sentis M., Martinuzzi S., Vervisch V., Torregrosa F., Etienne H., Roux L., Bastide S. *Proc. SPIE*, **6881**, 68811 (2008).
3. Vorobyev A.Y., Guo C. *Opt. Express*, **19**, A1031 (2011).
4. Zorba V., Persano L., Pisignano D., Athanassiou A., Stratakis E., Cingolani R., Tzanetakis P., Fotakis C. *Nanotechnology*, **17**, 3234 (2006).
5. Vorobyev A.Y., Guo C. *Opt. Express*, **18**, 6455 (2010).
6. Ionin A.A., Kudryashov S.I., Makarov S.V., et al. *Quantum Electron.*, **41**, 829 (2011) [*Kvantovaya Elektron.*, **41**, 829 (2011)].
7. Ma Y., Si J., Sun X., Chen T., Hou X. *Appl. Surf. Sci.*, **331**, 905 (2014).
8. Godbole V.P., Chaud Bari C.S. *Bull. Mater. Sci.*, **11**, 97 (1988).
9. Banishev A.F., Golubev V.S., Kremnev A.Yu. *Zh. Tekh. Fiz.*, **71**, 33 (2001).
10. Skvortsov A.M., Veiko V.P., Huynh C.T., Khaletskiy R.A. *Proc. SPIE*, **9065**, 90650S (2013).
11. Wai Lek Ng, Lourenco M.A., Gwilliam R.M., Ledain S., Shao G., Homewood K.P. *Nature*, **410**, 192 (2001).
12. Dittrich T., Timoshenko V.Y., Rappich J., Tsybeskov L. *J. Appl. Phys.*, **90**, 2310 (2001).

13. Skvortsov A.M., Veiko V.P., Huynh C.T. *Nauchno-Tekh. Vestn. Inf. Tekhnol., Mekh., Opt*., **81**, 128 (2012).
14. Skvortsov A.M., Veiko V.P., Huynh C.T., Petrov A.A. *Pis'ma Zh. Tekh. Fiz*., **41**, 65 (2015).
15. Polyakov D., Skvortsov A., Veiko V. *J. Laser Micro/Nanoeng*., **10**, 269 (2015).
16. Zangwill A. *Physics at Surfaces* (Cambridge: Cambridge University Press, 1988).
17. Iton M. *J. Phys. Condens. Matter*, **4**, 8447 (1992).
18. Duke C.B. *Chem. Rev.*, **96**, 1237 (1996).